RSC Advances

ROYAL SOCIETY OF CHEMISTRY

www.rsc.org/advances

Evolution of cellulose into flexible conductive green electronics: A smart strategy to fabricate sustainable electrodes for supercapacitors

Shilin Liu[a,b,c*], Tengfei Yu[c], Yuehan Wu[a], Wei Li[a], Bin Li[a]

a. College of Food Science & Technology, Huazhong Agricultural University, Wuhan, Hubei, 430070, China;

b. Jiangsu Province Biomass Energy and Materials Laboratary, Nanjing, Jiangsu, 210042 (China);

c. College of Chemical and Material Engineering, Jiangnan University, Wuxi, Jiangsu, 214122, China.

[*]Corresponding author: slliu2013@mail.hzau.edu.cn (S. Liu).

Abstract

The integration of native polymers with electronic elements to form green electronics will be the subject of intense scientific research. In this work, conductive cellulose composite films have been prepared by in situ polymerization of aniline monomers in the cellulose scaffolds. The effects of reaction time, different dopants and the concentration of aniline monomer on the structure and properties of the composite films have been investigated. With the optimized reaction protocols, the structurally defined polyaniline (PANI)/cellulose composite films with PANI content only about 24.6% exhibited electrical conductivity as high as 0.06 S•cm^{-1}, which could be compared with that of pure PANI. The PANI/cellulose films integrated the merits of cellulose and conductive polyaniline. The composite films with electrical conductivity performance were foldable and could be used as flexible electrode materials for supercapacitors. The specific capacitance of the films was about 120-160 F•g^{-1} at a current density ranging from 0.1 to 0.5 A•g^{-1} in the supercapacitor, and it kept at least 81% after 1000 cycles at current density of 0.5 A•g^{-1}. The straightforward fabrication of the cellulose-based conductive films represented not only a novel scientific term about supercapacitor-based energy storage materials, but also an emerging area of research aimed at identifying compounds of natural origin and establishing economically efficient routes for the production of environmentally safe (biodegradable) and/or biocompatible devices.

Keywords: cellulose, green electronics, conductive materials, supercapacitor

Introduction

Foldable electronic devices have been emerged for untraditional applications, and a certain amount of mechanical flexibility is preferred or required, such as roll-up displays, implantable medical devices and wearable devices, etc.[1-5] To fully realize flexible electronics, flexible energy storage devices are required. Supercapacitor is considered to be an extremely attractive alternative to rechargeable batteries because it exhibit several unique properties.[6-8] The active electrode materials for a supercapacitor mainly involve carbon materials,[9-11] transition metal oxides[12-15] and conductive polymer materials.[16-19] However, there is still a great challenge to fabricate flexible supercapacitor due to the lack of reliable electrodes that possess excellent electrical conductivity and high mechanical flexibility for high storage capacity and cycling performance in electrochemical environments. It has been observed that the electrode materials often suffer from mechanical crack owing to the delicate or fragile nature of metal oxide–based nanostructures. Development of freestanding anode and cathode with favorable mechanical strength and flexibility is in great demand for flexible and bendable energy storage devices.[20,21]

In recent years, the concerns over environmental pollution and depletion of fossil fuels have sparked the endeavors to develop alternative energy conversion/storage systems with high specific power and energy.[22-24] The integration of native polymers with electronic elements to form green electronics will be the subject of intense scientific research.[25] We have put an intensive research on cellulose dissolving and construction of functional cellulose materials from the developed solvent. In our previous works, aqueous solvents containing alkaline and urea have been developed for cellulose dissolving.[26,27] The regenerated cellulose films prepared from LiOH/urea or NaOH/urea aqueous solution had porous structure, it could be used as scaffolds for

the synthesis of inorganic nanoparticles[28-32] or curable organic prepolymers[33,34] in situ for the construction of functional cellulose materials. Inspired by this interesting phenomenon, in this work, a facile pathway has been presented to prepare conductive cellulose materials by using aniline monomer and porous structured cellulose scaffolds through in situ polymerization. We found the content of polyaniline had an obvious influence on the electrical conductivity of the composite films. The conductive films integrated the merits of cellulose and conductive polyaniline, and the composite films with polyaniline content only about 24.6 wt% exhibited electrical conductivity as high as 0.06 S•cm^{-1} and a specific capacitance of 120-160 F•g^{-1} at a current density ranging from 0.1 to 0.5 A• g^{-1} in the supercapacitor. The electrode made from the composite films had an excellent pseudocapacitance performance, including high specific capacitance and rate capability, good charge-discharge stability and long-term cycling life. It showcased acceptable electrochemical performance when used as electrodes for supercapacitor. Moreover, the performance of the device would be further improved once the conductivity of the composite film electrodes could be improved. This research may extend beyond supercapacitor-based energy storage and shed light on the future design of green electronics, which could help not only fulfill the original promise of organic electronics that is to deliver low-cost and energy efficient materials but also achieve unimaginable functionalities for electronics, for example benign integration into life and environment.

Experimental

Chemicals. Cotton linter pulp (α-cellulose > 95%, viscosity-average molecular weight was 1.03×10^5) was provided by Hubei Chemical Fiber Group Ltd (Xiangfan, China). Other chemicals with analytical grade were supplied by the Sinopharm Chemical Reagent Co. Ltd (China), aniline monomer was distilled doubly prior to use,

and other chemicals were used without further purification.

Preparation of regenerated cellulose (RC) film

The dissolving process for native cellulose has been reported in our previous work.[24] Briefly, Cotton linter pulp (native cellulose) was dispersed into aqueous LiOH/urea solution, and froze at -20 $^{\circ}$C to get a solid substance, then, thawed it at room temperature to obtain cellulose solution (5 wt%). After the removal of the bubbles in the solution by centrifugation, the solution was cast on a glass plate with the thickness about 1 mm, and then immersed it into anhydrous ethanol for coagulation and regeneration. The obtained RC films were washed with deionized water thoroughly and then kept in deionized water before using.

Preparation of polyaniline (PANI)/cellulose films by using HCl as doping agent

In a typical procedure, aniline monomer was dissolved in HCl solution (0.1 mol•L^{-1}), and then the RC films after treated with HCl solution (0.1 mol•L^{-1}) were immersed into it, the aniline monomer could permeate into the cellulose scaffolds through diffusion. Ammonium persulfate solution (1.0 mol•L^{-1}) was added dropwise to the solution containing RC films, the aniline monomers was oxidatively polymerized at 4 $^{\circ}$C for 4 hrs, and the color of the RC films turned from colorless into dark green. The composite films were washed with deionized water thoroughly, and then dried at ambient conditions. The composite films prepared from aniline with concentration of 0.01, 0.03, 0.05, 0.07 and 0.11 mol•L^{-1} was coded as RC/PA001, RC/PA003, RC/PA005, RC/PA007, RC/PA011, respectively. In order to clarify the effects of the polymerization time on the content of the polyaniline in the cellulose matrix, aniline (0.11 mol•L^{-1}) and HCl (0.1 mol•L^{-1}) were used in this progress, the method was similar to the mentioned above, but different polymerization time (0.5h, 1h, 2h, 3h, 4h) was carried out when the ammonium persulfate solution was added.

It was well known that the doping agent has an important influence on the conductivity of the polyaniline, in this work, different doping agents including HCl, H_2SO_4, H_3PO_4 and HNO_3 was used. In the polymerization process, the method was similar to the mentioned above, except the concentration of the used aniline and polymerization time were kept as 0.11 $mol \cdot L^{-1}$ and 7h, respectively. The concentration of the HCl, H_2SO_4, H_3PO_4 and HNO_3 was 0.1 $mol \cdot L^{-1}$, 0.05 $mol \cdot L^{-1}$, 0.033 $mol \cdot L^{-1}$, and 0.1 $mol \cdot L^{-1}$, respectively. The volume of the acid used was same.

Characterization

X-ray diffractometry of the RC and composites was carried out on reflection mode (Rigaku RINT 2000, Japan) with Ni-filtered CuKa radiation. Thermal gravimetric analysis (TGA) was performed on a thermogravimetric analysis (Ulvac TGD 9600). The samples were cut into powders and about 30 mg of the powder was placed in a platinum pan and heated from 20 to 700 ^{o}C at a rate of 10 $k \cdot min^{-1}$ in nitrogen atmosphere. Nitrogen adsorption-desorption measurements were performed with a Quantachrome NOVA 4200e (USA). Scanning electron microscopy (SEM) observation of the surfaces of the RC and composites was carried out by using a Hitachi S-4800 microscope. Prior to analysis, samples were cut into small pieces and coated with a thin layer of evaporated gold. The mechanical properties of the samples were characterized with a tensile tester (CMT 6503, Shenzhen SANS Test machine Co. Ltd, China) according to ASTM/D638-91, the crosshead speed was kept constant at 1 $mm \cdot min^{-1}$.

The conductivity of the samples was characterized with a conventional four-point probe technique (RTS-8, Probes Tech., China) at 25 ^{o}C. According to the fourpoint probe method, resistivity could be calculated with $\rho = 2\pi s \, (\, V \, / \, I \,)$, where S was the distance between the probes (mm), which was kept constant, I was the supplied

current in microamperes, and the corresponding voltage was measured in millivolts. Conductivity was calculated by using $\sigma = 1/(\rho \bullet X)$. In this process, five replicates for each sample were performed to obtain an average value.

Cyclic voltammetry and chronopotentiometry were carried out on a CHI660D electrochemical work station (Shanghai, China). Conventional three-electrode system was employed, involving glass carbon electrode as the working electrode, a platinum wire as the counter electrode and a saturated calomel electrode (SCE) as the reference electrode. The PANI/cellulose composites electrodes were prepared by dropcasting certain amounts of the dispersions on glassy carbon electrodes (dried at 40 °C). Cyclic voltammetry was performed in the voltage range from -0.2 to 0.8 V at 5, 10, 20, 30 and 50 mV$\bullet$s^{-1} scan rates in 1 mol$\bullet$L^{-1} H$_2$SO$_4$. The galvanostatic charge−discharge experiment was carried out in the potential range from -0.2 to 0.8 V with an applied current density of 0.2, 0.4, 0.6, and 0.8 A$\bullet$g^{-1}. The working electrode was prepared by mixing the active material with 15 wt% acetylene blank and 5 wt% polytetrafluoroeyhylene (based on the total electrode mass) to form a slurry. Then the slurry was cast on stainless steel mesh. Galvanostatic charge–discharge curves were measured in the potential range of -0.2–0.8 V at different current density. In this process, the PANI/cellulose composites were used as working electrode, and platinum foil (1 cm×1 cm) and a saturated calomel electrode (SCE) were used as the counter and reference electrode, respectively. The electrochemical measurements were carried out in a 6 mol$\bullet$L^{-1} potassium hydroxide aqueous electrolyte at room temperature.

Results and discussion

Morphology and structure of the RC and composite films

The process for the preparation of the PANI/cellulose films was shown in Schedule 1. The cellulose hydrogel film at swollen state had porous structure, comprising of

fibrils with the diameter about 20 nm, as it was shown in Fig. 1a. The porous structure was ascribed to the phase separation of the cellulose solution during the regeneration in ethanol, and the solvent-rich regions contributed to the formation of the pores. The water content and porosity of the obtained cellulose hydrogel film was respectively about 92% about 95%, and the S_{BET} of that was about 270 $m^2 \cdot g^{-1}$. When the RC film was immersed into aniline monomer solution, the aniline monomers could penetrate into the porous structured cellulose film through diffusion. The large amount of hydroxyl groups of cellulose could interact with amine groups of aniline to form the hydrogen bands which ensured the uniform distribution of aniline around the cellulose nanofibrils. The interaction between aniline and cellulose nanofibrils was a physical nature without involving chemical grafting. The aniline monomers polymerized in the cellulose matrix with the addition of the initiator. The composite films showed an obvious dark green color, suggesting the successful incorporation of PANI in the RC scaffolds. Fig. 1b-f shows the surface images of the PANI/cellulose composite films. The concentration of the aniline monomers had an obvious influence on the morphology of the composite films. For the composite films prepared from 0.01 $mol \cdot L^{-1}$ aniline, the cellulose nanofibrils were covered with continuous sheath of PANI, and some PANI particles were formed on the surface of the composite films, as it was shown in Fig. 1b. This process would be called dispersion polymerization, where the monomer in the polymerization was miscible with the reaction medium but the resulting polymer was not soluble, the PANI particles deposited in the cellulose scaffolds around the cellulose nanofibrils connected to form a continuous sheath by taking the cellulose nanofibrils network as templates. It must be noted that there was no PANI separated out from the reaction system when the color of the RC films turned into black green, indicating the macroscopic separation of the PANI was

prevented by the presence of the cellulose scaffolds. When the concentration of the aniline was 0.03 mol•L^{-1}, the composite films exhibited a denser structure when compared with RC/PA001, as it was shown in Fig. 1c. It indicated that the critical concentration of aniline was about 0.03 mol•L^{-1} for the full population of the pores in the cellulose matrix. When the concentration of aniline was further increased, the content of PANI particles increased with the precipitation or aggregation forming on the surface of the composite films (Fig. 1d-f). The PANI colloidal particles with particle size of 100-200 nm were polydisperse. It attested that the cellulose nanofibrils could act as templates for the polymerization of aniline in situ, and the hydrogen bands between cellulose nanofibrils and aniline served as traction force to assist the formation polyaniline colloidal particles around cellulose nanofibrils.

Based on the results from Fig. 1, the influence of the reaction time on the structure of the PANI/cellulose composite films has been investigated. Fig. 2 shows the images of the composite films prepared from different reaction time with aniline concentration of 0.11 mol•L^{-1}. The porous structured RC was filled with PANI particles within 30 mins, as it was shown in Fig. 2a. It demonstrated the polymerization process was very quick, which was important for the large-scale preparation of the cellulose based conductive materials. However, precipitation or aggregation of the PANI colloidal particles occurred to form larger dimension particles (Fig. 2c, d) with the extension of the reaction time, and the composite films prepared from longer polymerization time exhibited a denser structure. It indicated that the microstructure of the composite films could be controlled by changing the concentration of the aniline monomer or the polymerization time.

FT-IR spectrum was used to characterize the interactions between cellulose and PANI from molecular level, and it was shown in Fig. 3. In the case of pure RC, a

broad band at 3403 cm^{-1} was attributed to O-H stretching vibration. The band at 2897 cm^{-1} represented the aliphatic C-H stretching vibration. A sharp and steep band observed at 1068 cm^{-1} was due to the presence of C-O-C stretching vibrations.[35] It was worth noting that the peak at 1647 cm^{-1} was ascribed to the carbonyl functional groups as a result of natural aging of cellulose. In the case of PANI/cellulose composites, the band at 3403 cm^{-1} and 1647 cm^{-1} became weaker with the increasing content of PANI, indicating the cellulose scaffold was sufficiently coated with PANI, and the result had been confirmed by the data from SEM. Further evidence of PANI coated onto cellulose scaffolds could be found in the disappearance of the sharp band at 2897 cm^{-1}, which was assigned to the aliphatic C-H stretching vibration. Moreover, the characteristic bands of PANI in PANI/cellulose composites were clearly observed at 1579 and 1498 cm^{-1}, which were assigned to the C-C stretching of the quinoid and benzenoid rings, respectively.[36] In addition, the bands at 1297, 1154, and 813 cm^{-1} were correlated to the C-N in-plane ring bending modes, the C-H in-plane bending, and the C-H out-of-plane bending modes, respectively. All the results indicated that the PANI component was incorporated into cellulose scaffolds.

Fig. 4 shows the XRD of the RC, PANI and PANI/cellulose composite films. The peaks at 2θ = 12.1, 20.3, and 21.8° were corresponded to the (1$\bar{1}$0), (110), and (200) planes of cellulose II crystalline, respectively.[37] Two broad peaks at 20.4°, and 25.2 $^{\circ}$ were observed for PANI[38], and the degree of crystallinity of the PANI synthesized through the same way was relatively low. The chemical structure of RC was remained unchanged for the composite films, suggesting the polymerization happened in the aniline monomers, and the cellulose scaffolds was just as templates for the stabilization of the synthesized PANI particles. Based on our previous works, it was worth noting that the porous structured RC film was a fascinating template for the

construction of functional materials through in situ polymerization of polymer monomers, besides for the synthesis of inorganic nanoparticles or cured some organic prepolymers in situ.

Thermal, mechanical and electrochemical properties of the composites

The thermal stability of the RC and the PANI/cellulose composites was investigated by using thermogravimetry in N_2 atmosphere, and the date was shown in Fig. 5a. All the materials exhibited excellent heat-resistance up to at least 200 °C. There was a small weight loss of ~5% below 100 °C for the RC and composites, which was ascribed to the release of the moisture from the samples. With the elevating temperature, the pure RC film showed an obvious weight loss in the temperature ranging from 300~350 °C, which was the decomposition temperature of cellulose in N_2. The thermal stability of the composites decreased with the incorporation of PANI, the composites experienced a sharp weight loss from 200 to 600 °C. The TG curve of pure RC showed that it also experienced a similar weight loss process. However, the onset temperature of the thermo-oxidative degradation of the RC was 120 °C higher than that of the PANI/cellulose composites, indicating that the thermal stability of the PANI/BC composite was lower than that of untreated RC, but the thermal stability of the PANI/cellulose composites was similar to that of the pure PANI.[39] The final step in weight loss was observed from 600 to 800 °C, which was resulted from the thermal-oxidative degradation of PANI and the RC. The residue obtained from the thermal gravimetric curves increased with the increasing of the concentration of aniline solution, indicating the content of the resulted PANI in the cellulose matrix increased with the increasing of the concentration of the monomer, and the data was shown in Fig. 5b.

Preparation of PANI/RC composite films for the highest electrical conductivity was

optimized by sequentially tuning the reaction parameters including the concentration of the aniline monomer, polymerization time, and different dopants. Fig. 6a shows the effects of the concentration of aniline monomer on the PANI content and the conductivity of the composite films. The concentration of the aniline monomers had an obvious influence on the conductivity of the composite films, and it demonstrated that the conductivity of the composite films was correlated to the content of PANI. For the composite films prepared from aniline monomer with concentration of 0.05 mol•L^{-1}, the conductivity of the composite films was about 6.2×10^{-4} S•cm^{-1}, and the content of the PANI was about 15 wt%. When the concentration of the aniline monomer was up to 0.11 mol•L^{-1}, the PANI content and the conductivity of the composite films could be observed and the values are 24.6 wt% and 0.06 S•cm^{-1}, respectively. It must be noted that the conductivity of pure cellulose and PANI film doped with HCl was about 2×10^{-11} and 0.4 S•cm^{-1}, respectively.[40]Some researchers have explored the preparation of bacterial cellulose/PANI conducting nanocomposites by in situ polymerization of aniline nanoparticles onto bacterial cellulose films to obtain electrical conductivity ranging from 2×10^{-4} to 5.1 S•cm^{-1},[39-41] and the composite films with higher conductivity should have higher content of PANI. In the work, the biomass based composite film with 24.6 wt% PANI had electrical conductivity as high as 0.06 S•cm^{-1}. It was worth noting that cellulose as the most abundant native polymer had excellent mechanical properties, nevertheless, poor performance in technical applications. However, the unique chemical structure of cellulose would provide a good platform for the construction of new biomaterials and biodevices. Indeed, the high density of free hydroxyl groups in the cellulose structure made it a helpful solid substrate that could undergo functionalization allowing the production of new materials for novel advanced applications. As far as we know, the

conductive performance for cellulose based composites containing content of PANI lower than 25 wt% has not been reported previously. Furthermore, the conductivity of the PANI/cellulose composite films could also be improved by loading PANI with higher content, but the mechanical performance of the composite films would be decreased. The influence of the reaction time on the electrical conductivity was shown in Fig. 6b. The electrical conductivity of the composite films increased with the increasing of the reaction time, and tended to a plateau after 4 hours. It would be ascribed to the incorporated PANI at this time, which allowed the formation of continuous conducting layers on the cellulose nanofibrils' surface. These results revealed that the needed reaction time for the preparation of PANI/cellulose conductive films with higher electrical conductivities at 0.11 mol$\cdot$L^{-1} aniline concentration and 0.1 mol$\cdot$L^{-1} HCl was about 4 h. The influence of the different acids on the electrical conductivity of the PANI/cellulose composite films was shown in Fig. 6c. The PANI/cellulose films doped with HCl had the highest electrical conductivity of 0.06 S$\cdot$cm^{-1}, when doped with H_2SO_4 solution, the electrical conductivity was decreased to 0.053 S$\cdot$cm^{-1}, and the composite films doped with H_3PO_4 had the lowest conductivity, and it should be due to the fact that stronger acid usually produce enough protonic hydrogen with the higher degree of ionization, which assured the favorable electrical conductivity of the doped PANI with the same concentration of the acid and oxidant. However, H_2SO_4 and H_3PO_4 cannot ionize completely, and hydrogen sulfate and hydrogen phosphate anions were exclusively presented in PANI/H_2SO_4 and PANI/ H_3PO_4.[42] Therefore, in the same concentration of hydrogen ion in protonic acids, the electrical conductivity of the prepared composite films was: $HCl > H_2SO_4 > HNO_3 > H_3PO_4$.

To investigate the mechanical characteristics of PANI/cellulose films, the tensile

test was performed. The tensile behavior of the RC and PANI/cellulose films was shown in Fig. 7. The Young's modulus and tensile strength of RC were 2.2 GPa and 73 MPa, respectively. The tensile strength and Young's modulus for the RC/PA001 increased slightly with the low content of the PANI in the composites. The stress decreased with the increasing content of PANI in the composite films, and as expected, the Young's modulus of the composite films increased firstly and then decreased. The Young's modulus of the RC/PA011 film with 24.6 wt % PANI was around 1.8 GPa and tensile strength around 53 MPa. This decreased behavior of PANI/cellulose films in stress would be associated with the weakened inter- and intramolecular hydrogen bonding of cellulose caused by the introduction of PANI. It was obvious that the composite films overcame the limitation of preparation for conductive film from pure PANI, which also combined the excellent mechanical properties of the cellulose. The obtained composite films were foldable, and had good mechanical properties and favorable conductivity, which could be used as a promising material in the application of sensors, flexible electrodes, display devices, and other electrically conductive flexible film fields.

Conductive composites for flexible supercapacitors

Potential applications of the PANI/cellulose films were explored by development the composites into supercapacitor electrodes and characterizing the cyclic voltammograms (CVs) and galvanostatic charge/discharge performance. Fig. 8a shows the CVs of the PANI/cellulose films prepared from different concentration of aniline monomers. The CV curves of the RC/PA001 and RC/PA003 was a nearly horizontal straight line without any redox peaks, which manifested that they only possessed a negligible electrical double-layer capacitance, because of the poor electrical conductivity. However, the capacitance characteristics of the RC/PA005,

RC/PA007 and RC/PA011 were distinct from that of the electric double-layer capacitance and close to the ideal rectangular shape with pseudocapacitance characteristics. The PANI/cellulose composite films with conductivity higher than 6.2 $\times 10^{-4}$ S•cm^{-1} had three pairs of redox peaks: the first couple of peaks (about 0.21 V/0.10 V) was attributed to the redox transition of PANI between a semi-conducting state (leucoemeraldine form) and a conducting state (polaronicemeraldine form); the second couple of peaks (about 0.48 V/0.44 V) was due to the transformation between the *p*-benzoquinone/hydroquinone couple because of the attack by water; the third couple of peaks (about 0.76 V/0.70 V) was correlated to the formation/reduction of bipolaronic pernigraniline and protonated quinonediimine.[43-45] It was found that the CV curve area of PANI/cellulose composite films increased with the increasing the content of PANI in the composite films. The presence of cellulose as a template in the polymerization system could lead to the change in the morphology of PANI, and the cellulose itself did not contribute to the electrical capability. Therefore, the increase in the CV curve area was ascribed to the PANI components. The CV curve area of the RC/PA005, RC/PA007 and RC/PA011 composite films increased with the increasing content of PANI in the composite films. Furthermore, the first and third couples of peaks of the RC/PA005, RC/PA007 and RC/PA011 composite films were obvious, and it indicated that RC/PA005, RC/PA007 and RC/PA011 composite films would have a higher specific capacitance because of the linear relation between specific capacitance and CV curve area. Fig. 8b shows the CV curves for the RC/PA011 electrodes at various scan rates. CV curve area increased with increasing scan rate. It was reported the pseudocapacitance of PANI was due to the redox reaction involving in the influx and outflow of counter ions from the polymer. Therefore, the CVs of the RC/PA011 composite represented the reversible

redox processes. Three pairs of redox peaks were observed in the curve even at scan rates to 50 mV• s^{-1}. The first couple of peaks were significantly high, and the third couple of peaks were relatively flat but visible yet, indicating the RC/PA011 composites had a good electrochemical stability.

Fig. 9a shows the charge/discharge curves of the RC/PA011 composite electrode at various current densities of 0.1, 0.2, 0.3, 0.4, and 0.5 A•g^{-1}. The charge curves were almost linear and symmetrical to their discharge counterparts, indicating good electrochemical performance of the RC/PA011 composite electrode. The specific capacitance of the electrode could be calculated using the following equation:[46]

$$C_{\mathrm{m}} = (It) \big/ (\mathrm{V}Vm)$$

where C_m was specific capacitance (F•g^{-1}), I was charge/discharge current (A), t was the time of discharge (S), ΔV was the voltage difference between the upper and lower potential limits, and m was the mass of the active electrode material. According to the above equation, the gravimetric capacitance of the RC/PA011 composite electrode at various current densities was plotted in Fig. 9b. Specific capacitance values as high as 120-160 F•g^{-1} were obtained at a current density ranging from 0.1 to 0.5 A• g^{-1}, which were comparable to that of pure PANI film (150 F/g)[47] and polyaniline/titanium nitride nanotube hybrid (194 F/g).[48] The high C_m would be attributed to the good dispersion of PANI coating around cellulose nanofibrils, which could help to provide a largely electrolyte-accessible surface area to improve utilization of PANI particles for redox reactions.

The long cycle life of supercapacitors is also a crucial parameter for their practical application. Fig. 10a shows the typical galvanostatic charge-discharge tests of the RC/PA011 composite electrode within the potential window of -0.2-0.8 V at a current density of 0.5 A• g^{-1}. Each charge–discharge cycle had a very similar potential-time

response behavior, which also implied that the charge–discharge process was reversible. The discharge specific capacitance of the RC/PA011 composite electrode was up to 120 F•g^{-1} at a current density of 0.5 A• g^{-1}. Moreover, cyclic performances of the RC/PA011 composite electrode were also examined by galvanostatic charge–discharge tests for 1000 cycles. Fig. 10b shows the capacitance kept at least about 81% after 1000 cycles at current density of 0.5 A• g^{-1}. The results demonstrated that the RC/PA011 composite electrode offered an excellent pseudocapacitance performance, including high specific capacitance and rate capability, good charge–discharge stability and long-term cycling life. This should be attributed to the intermolecular interaction between the PANI chains and the cellulose nanofibril templates, and it restricted the change of the nanostructure. Therefore, the RC/PA011 composite film electrode exhibited an excellent cycling stability. It was worth noting that when the cellulose scaffolds just contained 25 wt% PANI, the composite films showcased acceptable electrochemical performance levels when used as electrodes for supercapacitor. Moreover, the device performance would be further improved once the conductivity of the cellulose based film electrodes was improved. We hope this work would open a new research interesting on green electronics aiming at identifying compounds of natural origin and establishing economically efficient routes.

Conclusions

The novel conductive PANI/cellulose composite films have been successfully synthesized in situ by oxidative polymerization of aniline using cellulose scaffolds as the templates. The structure and properties of the composite films evolved strongly with the reaction parameters including the concentration of the aniline monomer, reaction duration, and different dopants. For the composite films prepared from aniline solution with lower concentration, the PANI uniformly deposited on the

cellulose scaffolds forming a continuous nanosheath by taking along the cellulose nanofiberils as template. With the increasing concentration of the aniline, more and more PANI particles were uniformly deposited on the surface of the composite gels. With the optimized reaction protocols, the structurally defined PANI/cellulose composite films exhibited outstanding electrical conductivity (ca. 0.06 S•cm^{-1}) and good mechanical properties. The as-prepared PANI/cellulose composite films had a specific capacitance hitting 160 F•g^{-1} at 0.1A•g^{-1} current density in the supercapacitor, which would be feasible in applications that require high power. The composite films integrated the merits of cellulose and conductive polyaniline. The importance of the electric conductivity, thermal stability, well-controlled microstructure and the performance of the composite films were investigated to pave the way toward promising applications in various electronic devices, which would offer insights for green electronics development. Moreover, the approach described in this work had great potential to tailor the functionality and to improve the performance of cellulose material, it might open the whole range of composite manufacturing technologies relying on in situ polymerizing matrices.

Notes and references

1. Y. Liu, H. L. Zhou, R. Cheng, W. J. Yu, Y. Huang, X. F. Duan, *Nano Lett.*, 2014, **14**, 1413-1418.

2. X.W. Wang, Y. Gu, Z. P. Xiong, Z. Cui, T. Zhang, *Adv. Mater.*, 2014, **26**, 1336-1342.

3. O. Bubnova, Z. U. Khan, H. Wang, S. Braun, D. R. Evans, M. Fabretto, P. Hojati-Talemi, D. Dagnelund, J. B. Arlin, Y. H. Geerts, *Nat. Mater.*, 2014, **13**, 190-194.

4. Y. Ji, D. F. Zeigler, D. S. Lee, H. Choi, A. K. Y. Jen, H. C. Ko, T. W. Kim, *Nat. Commun.*, 2013, **4**, 2707.

5. Z. Shi, H. Guo, J. Feng, B. Ding, X. Cao, S. Kuga, Y. Wang, L. Zhang, J. Cai, *Angew. Chem. Int. Ed.,*2014, **53**, 5380-5384.

6. Y. G. Wang, Y. Y. Xia, *Adv. Mater.*, 2013, **25**, 5336-5342.

7. M. Biswal, A. Banerjee, M. Deo, S. Ogale, *Energy Environ. Sci.*, 2013, **6**, 1249-1259.

8. Y. B. Tan, J. M. Lee, *J. Mater. Chem. A*, 2013, **1**, 14814-14843.

9. Z. Li, Z. W. Xu, H. L. Wang, J. Ding, B. Zahiri, C. M. B. Holt, X. H. Tan, D. Mitlin, *Energy Environ. Sci.*, 2014, **7**, 1708-1718.

10. C. Choi, J. A. Lee, A. Y. Choi, Y. T. Kim, X. Lepro, M. D. Lima, R. H. Baughman, S. J. Kim, *Adv. Mater.*, 2014, **26**, 2059-2065.

11. S. Han, D. Q. Wu, S. Li, F. Zhang, X. L. Feng, *Adv. Mater.*, 2014, **26**,849-864.

12. S. Giri, D. Ghosh, C. K. Das, *Adv. Funct. Mater.*, 2014, **24**,1312-1324.

13. W. W. Zhou, D. Z. Kong, X. T. Jia, C. Y. Ding, C. W. Cheng, G. W. Wen, *J. Mater. Chem. A*, 2014, **2**, 6310-6315.

14. K. M. Hercule, Q. L. Wei, A. M. Khan, Y. L. Zhao, X. C. Tian, L. Q. Mai, *Nano*

Lett., 2013, **13**, 5685-5691.

15. H. W. Shim, A. H. Lim, J. C. Kim, E. Jang, S. D. Seo, G. H. Lee, T. D. Kim, D. W. Kim, *Sci. Rep.*, 2013, **3**, 2325.

16. S. B. Kulkarni, U. M. Patil, I. Shackery, J. S. Sohn, S. Lee, B. Park, S. Jun, *J. Mater. Chem. A*, 2014, **2**, 4989-4998.

17. Z. Tong, Y. Yang, J. Wang, J. Zhao, B. L. Su, Y. Li, *J. Mater. Chem. A*, 2014, **2**, 4642-4651.

18. B. N. Reddy, M. Deepa, A. G. Joshi, *Phys. Chem. Chem. Phys.*, 2014, **16**, 2062-2071.

19. Y. Shi, L. J. Pan, B. R. Liu, Y. Q. Wang, Y. Cui, Z. A. Bao, G. H. Yu, *J. Mater. Chem. A*, 2014, **2**, 6086-6091.

20. J. W. Park, S. J. Park, O. S. Kwon, C. Lee, J. Jang, J. W. Park, S. J. Park, C. Lee, O. S. Kwon, *Chem. Mater.*, 2014, **26**, 2354-2360.

21. H. J. Lin, L. Li, J. Ren, Z. B. Cai, L. B. Qiu, Z. B. Yang, H. S. Peng, *Sci. Rep.*, 2013, **3**. 1353.

22. R. F. Service, *Science.*, 2013, **340**, 1162-1165.

23. C. Schmidt, *Nature.*, 2012, **483**, S37-S37.

24. A. Noy, *Adv. Mater.*, 2011, **23**, 807-820.

25. M. Irimia-Vladu, *Chem. Soc. Rev.*, 2014, **43**,588.

26. S. Liu and L. Zhang, *Cellulose.*, 2009, **16**, 189-198.

27. J. Zhou, S. Liu, J. Qi and L. Zhang, *J. Appl. Polym. Sci.*, 2006, **101**, 3600-3608.

28. S. Liu, L. Zhang, J. Zhou and R. Wu, *J. Phys. Chem. C.*, 2008, **112**, 4538-4544.

29. S. Liu, J. Zhou, L. Zhang, J. Guan and J. Wang, *Macromol. Rapid Commun.*, 2006, **27**, 2084-2089.

30. S. Liu, L. Zhang, J. Zhou, J. Xiang, J. Sun and J. Guan, *Chem. Mater.*, 2008, **20**,

3623-3628.

31. S. Liu, J. Zhou and L. Zhang, *J. Phys. Chem. C*, 2011, **115**, 3602-3611.

32. S. Liu, Q. Yan, D. Tao, T. Yu and X. Liu, *Carbohydr. Polym.*, 2012, **89**, 551-557.

33. S. Liu, D. Tao, T. Yu, H. Shu, R. Liu and X. Liu, *Cellulose.*, 2013, **20**, 907-918.

34. W. Li, Y. Wu, W. Liang, B. Li and S. Liu, *ACS Appl. Mater. Interfaces.*, 2014, **6**, 5726-5734.

35. C. J. Grande, F. G. Torres, C. M. Gomez and M. Carmen Bañó, *Acta Biomater.*, 2009, **5**, 1605-1615.

36. S. M. Ebrahim, A. Kashyout and M. Soliman, *J. Polym. Res.*, 2007, **14**, 423-429.

37. L. Zhang, D. Ruan and J. Zhou, *Ind. Eng. Chem. Res.*, 2001, **40**, 5923-5928.

38. T. Abdiryim, R. Jamal, I. Nurulla, *J. Appl. Polym. Sci.*, 2007, **105**, 576-584.

39. A. Youssef, S. Kamel, M. El-Sakhawy and M. El Samahy, *Carbohydr. Polym.*, 2012, **90**, 1003-1007.

40. Z.-l. Mo, Z.-l. Zhao, H. Chen, G.-p. Niu and H.-f. Shi, *Carbohydr. Polym.*, 2009, **75**, 660-664.

41. H. Wang, E. Zhu, J. Yang, P. Zhou, D. Sun and W. Tang, *J. Phys. Chem. C.*, 2012, **116**, 13013-13019.

42. M.-H. Qu, Y.-Z. Wang, C. Wang, X.-G. Ge, D.-Y. Wang and Q. Zhou, *Eur. Polym. J.*, 2005, **41**, 2569-2574.

43. Y. Li, X. Zhao, Q. Xu, Q. Zhang and D. Chen, *Langmuir.*, 2011, **27**, 6458-6463.

44. C.-C. Hu and C.-H. Chu, *J. Electroanal. Chem.*, 2001, **503**, 105-116.

45. C.-C. Hu and J.-Y. Lin, *Electrochim. Acta.*, 2002, **47**, 4055-4067.

46. A. L. M. Reddy and S. Ramaprabhu, *J. Phys. Chem. C.*, 2007, **111**, 7727-7734.

47. F. Fusalba, P. Gouérec, D. Villers and D. Bélanger, *J. Electrochem. Soc.*, 2001, **148**, A1-A6.

48. C. Xia, Y. Xie, Y. Wang, W. Wang, H. Du and F. Tian, *J. Appl. Electrochem.*, 2013, **43**, 1225-1233.

Table 1. Some properties of the RC and PANI/cellulose composite films.

Samples		PANI content (wt%)	S_{BET} (m^2/g)	Stress (MPa)	Strain (%)	Young's modulus (GPa)	Conductivity (S•cm^{-1})
	RC	0	--	73 ± 3.56	9.93 ± 0.43	2.22 ± 0.04	--
	RC/PA001	3.68	53	75 ± 4.09	7.42 ± 0.38	2.83 ± 0.07	--
Different concentration	RC/PA003	10.42	46	67 ± 3.41	7.36 ± 0.33	2.40 ± 0.09	--
	RC/PA005	15.17	40	47 ± 2.67	5.65 ± 0.21	2.17 ± 0.08	5.76×10^{-4}
	RC/PA007	21.05	36	54 ± 3.09	5.58 ± 0.19	1.78 ± 0.06	1.06×10^{-3}
	RC/PA011	24.61	25	53 ± 2.13	4.12 ± 0.16	1.81 ± 0.08	6.02×10^{-2}
Different dopants	HCl- PA011	24.61	25	53 ± 2.13	4.12 ± 0.16	1.81 ± 0.08	6.02×10^{-2}
	H_2SO_4- PA011	23.47	28	50 ± 3.17	4.67 ± 0.21	1.73 ± 0.06	5.23×10^{-2}
	HNO_3- PA011	22.67	34	49 ± 2.36	5.33 ± 0.24	1.83 ± 0.07	9.13×10^{-3}
	H_3PO_4- PA011	21.45	39	52 ± 2.18	5.46 ± 0.20	1.88 ± 0.07	4.76×10^{-4}
Different reaction time	HCl- PA011-0.5h	13.34	38	49 ± 2.67	6.19 ± 0.28	2.21 ± 0.08	1.97×10^{-2}
	HCl- PA011-1h	17.46	44	46 ± 2.82	5.42 ± 0.24	1.92 ± 0.06	2.28×10^{-2}
	HCl- PA011-2h	20.68	38	51 ± 2.09	5.36 ± 0.25	1.88 ± 0.04	4.78×10^{-2}
	HCl- PA011-4h	23.01	29	54 ± 1.87	4.81 ± 0.24	1.79 ± 0.06	5.68×10^{-2}
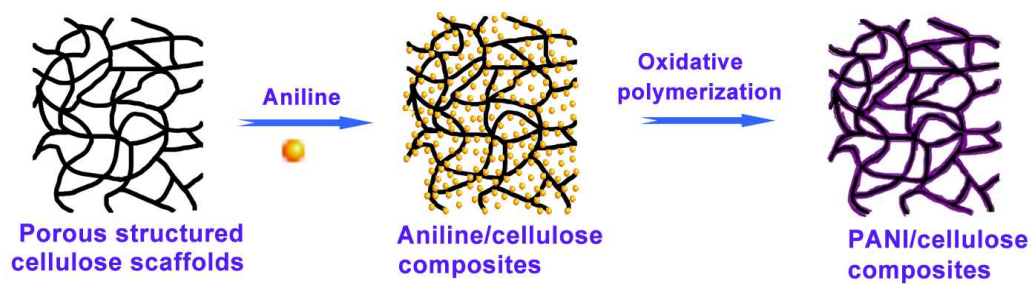
Schedule 1. Diagram for the preparation of conductive cellulose films by in situ polymerization of aniline in the presence of cellulose scaffolds.
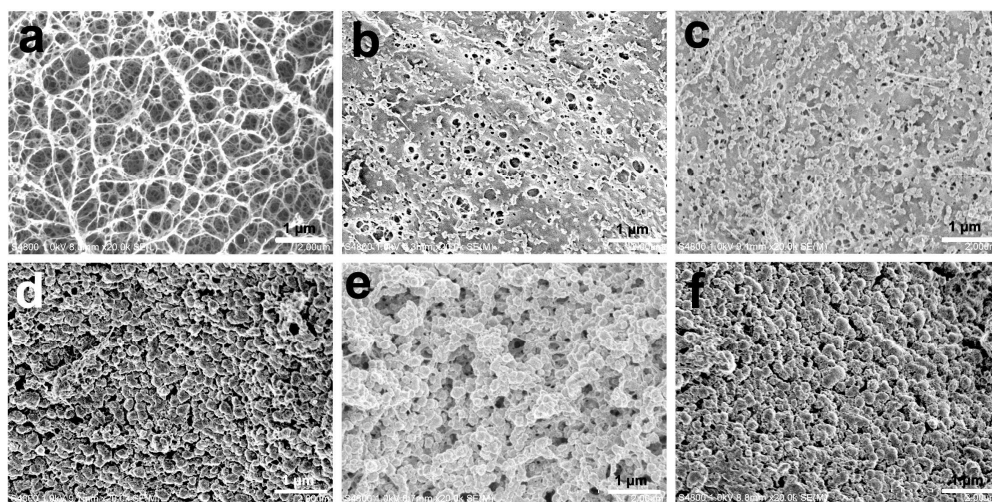
Fig. 1 FE-SEM images of surface morphologies of the pure RC (a) and the PANI/RC composites prepared from different concentration of aniline, (b) 0.01 mol•L^{-1}, (c) 0.03 mol•L^{-1}, (d) 0.05 mol•L^{-1}, (e) 0.07 mol•L^{-1}, and (f) 0.11 mol•L^{-1}, respectively. The polymerization time was 4 hours.
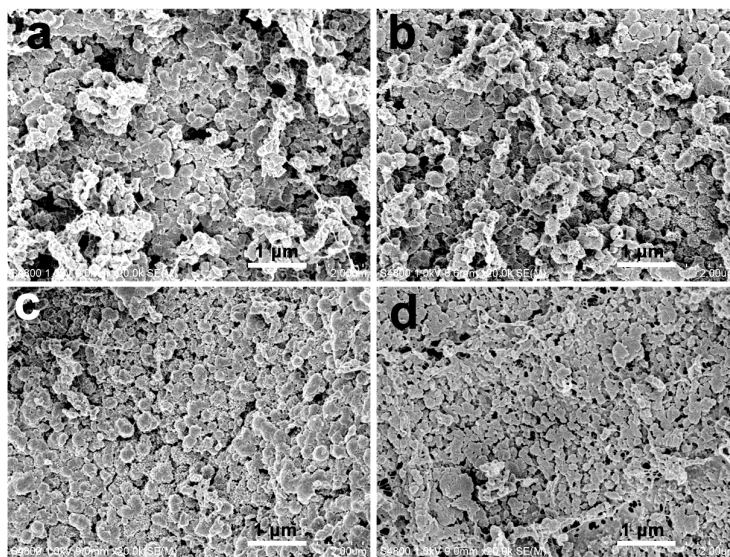
Fig. 2 FE-SEM images of the surface morphologies of the PANI/RC composites formed with the reaction time of (a) 0.5 h, (b) 1 h, (c) 2 h, and (d) 3 h, respectively. The concentration of aniline monomer was 0.11 mol·L^{-1}, HCl was used as dopant.
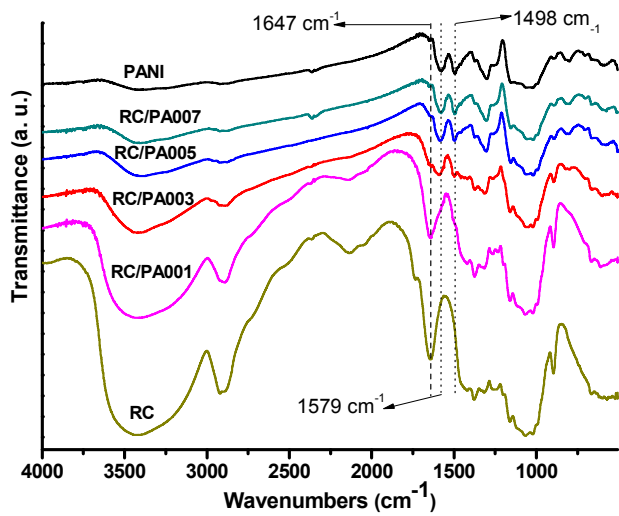
Fig. 3 FT-IR spectra of pure RC, PANI and PANI/cellulose composites.
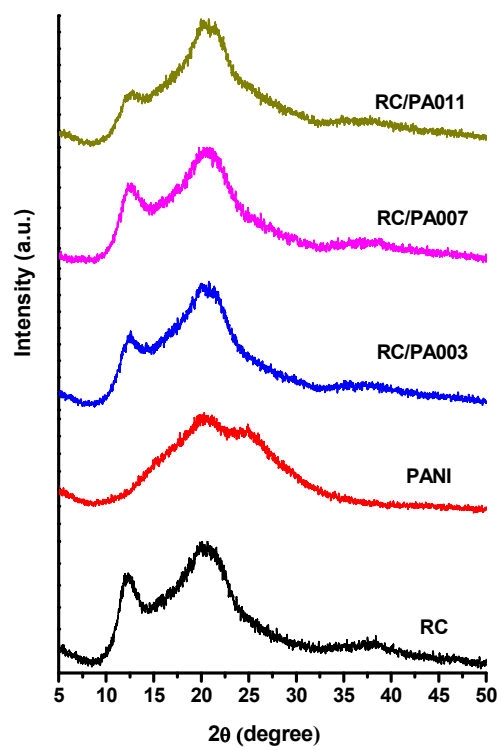
Fig. 4 XRD patterns of the RC, PANI and PANI/cellulose composites.
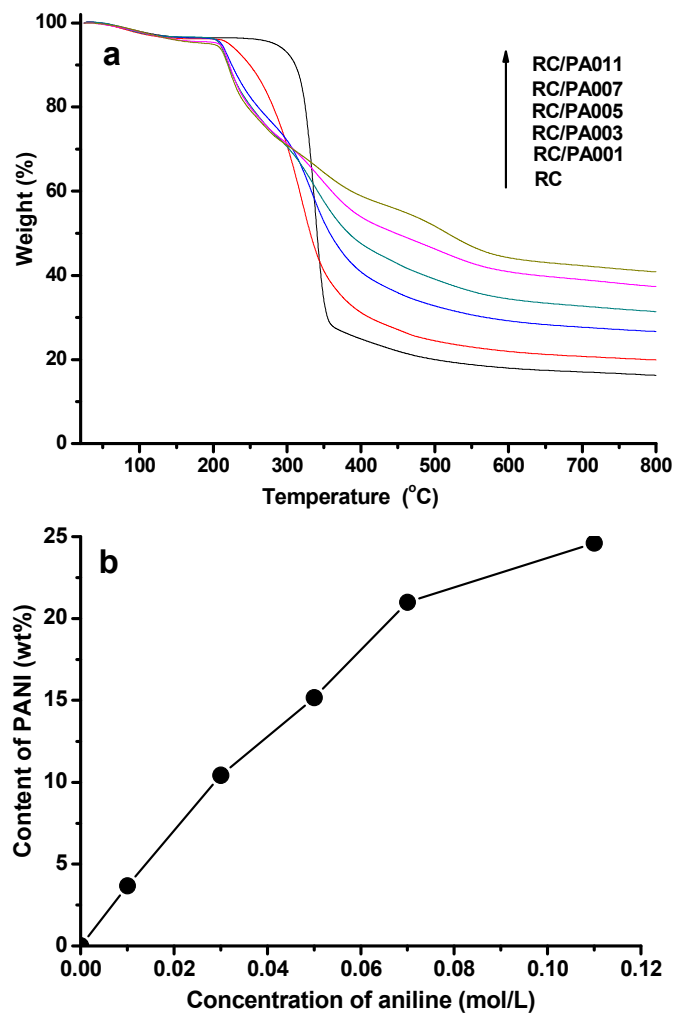
Fig. 5 TG curves (a) of the RC and PANI/cellulose composites, and the corresponding content of synthesized PANI in the composites deduced from the TG analysis (b).
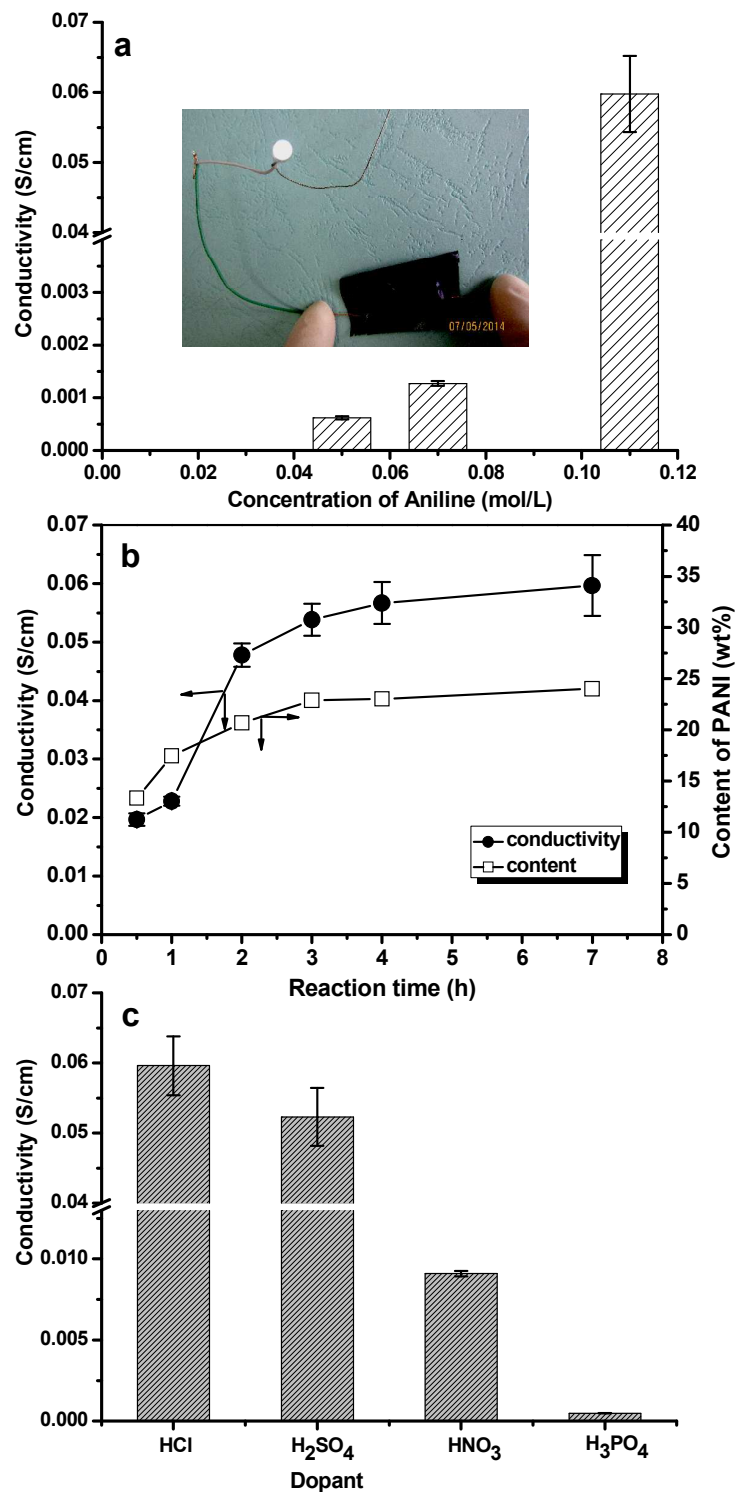
Fig. 6 Effect of the concentration of aniline monomer (a), different polymerization time (b), and different types of dopant on the electrical conductivity of the PANI/RC composite films, inserted was the conductive test photo of the composite film prepared from aniline with concentration of 0.07 mol·L^{-1}.
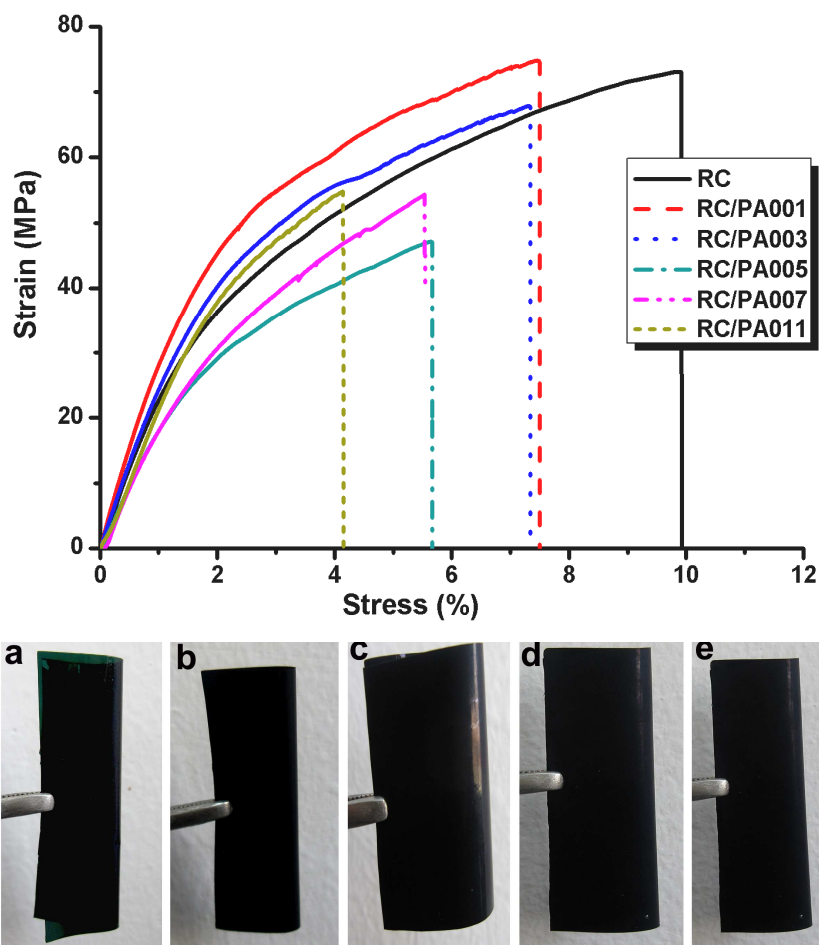
Fig. 7 Tensile stress strain behaviors of the RC and PANI/cellulose composite films (a), and the photos of the PANI/cellulose films that prepared from aniline with different concentration, a, b, c, d, e were for RC/PA001, RC/PA003, RC/PA005, RC/PA007 and RC/PA011, respectively.
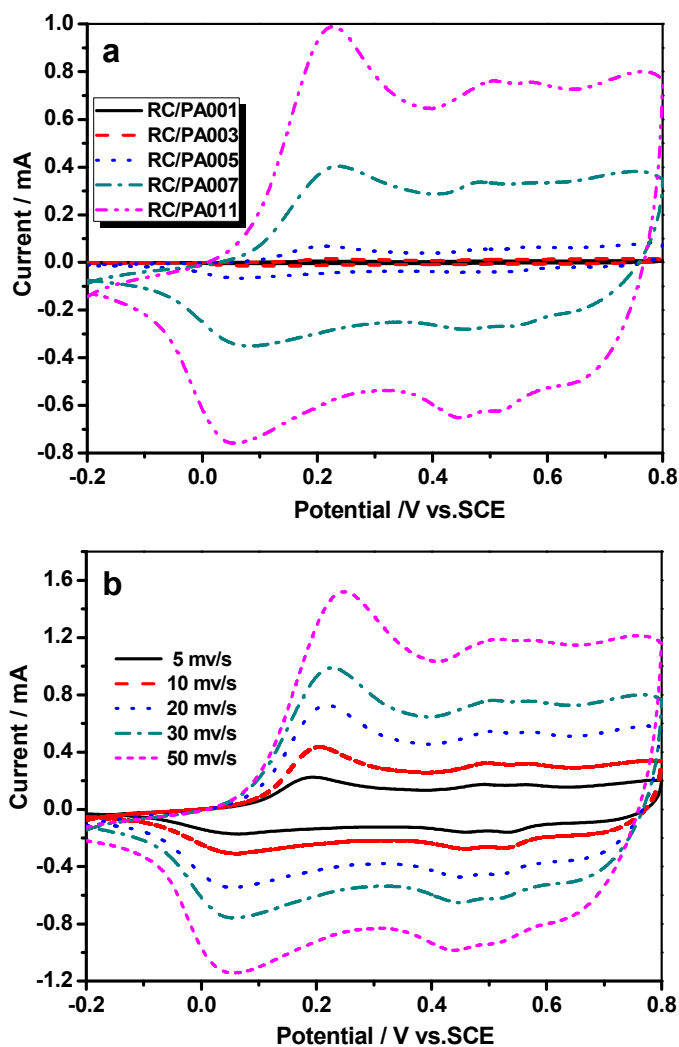
Fig. 8 Cyclic votammograms of the PANI/cellulose electrode at scan rate of 30 mv/s (a), and the RC/PA011 electrode at various scan rates in 1 M H_2SO_4(b).
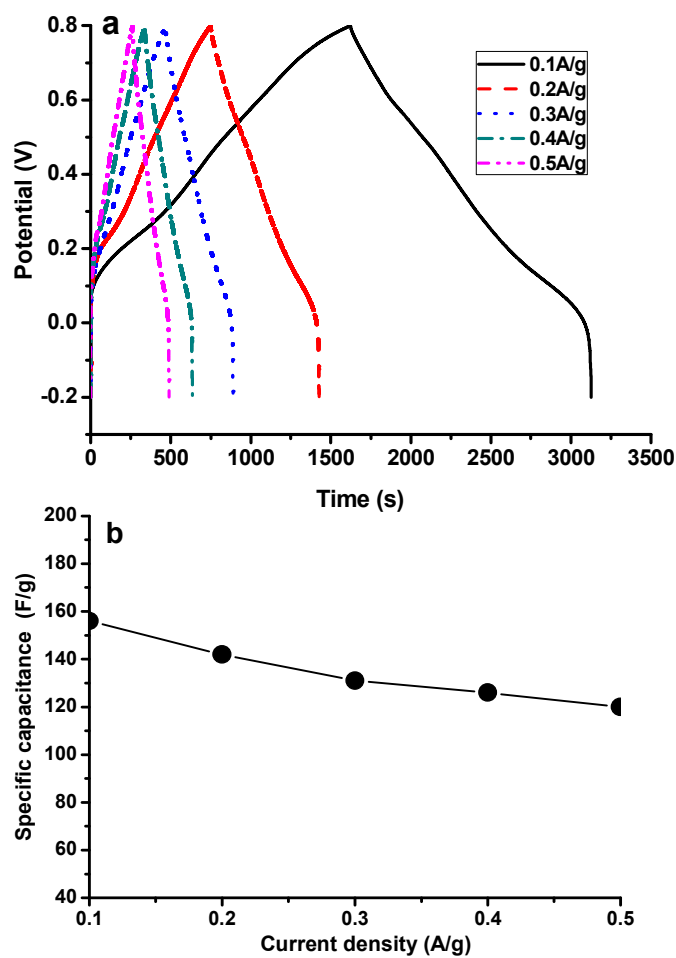
Fig. 9 Galvanostatic charge/discharge curves of RC/PA011 electrode at various current densities (a), and the corresponding discharge capacitances of RC/PA011 electrode at various current densities (b).
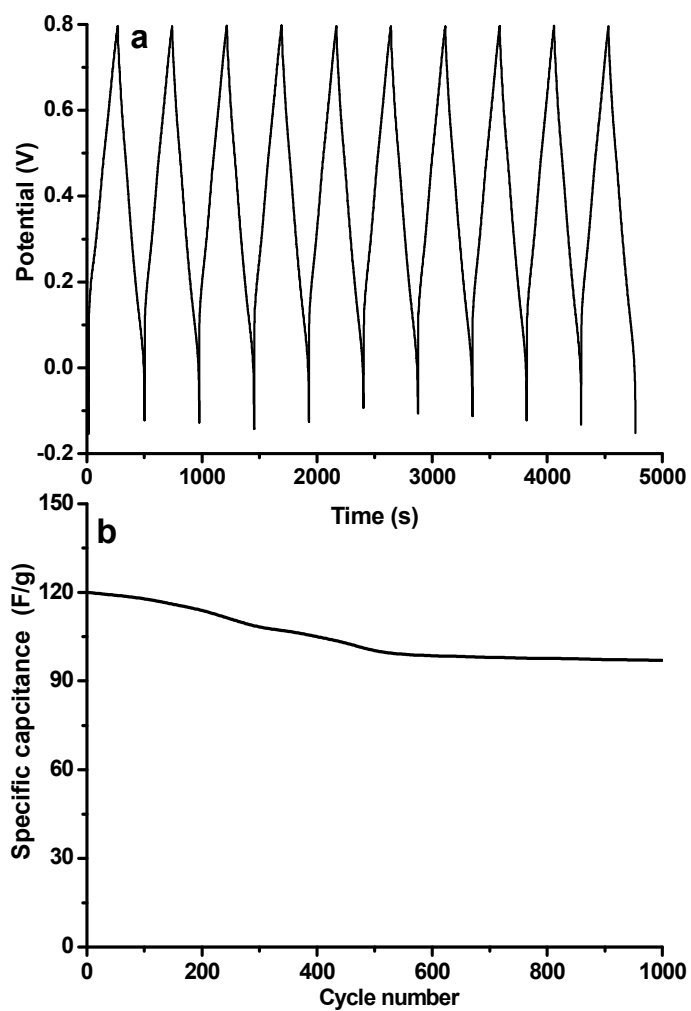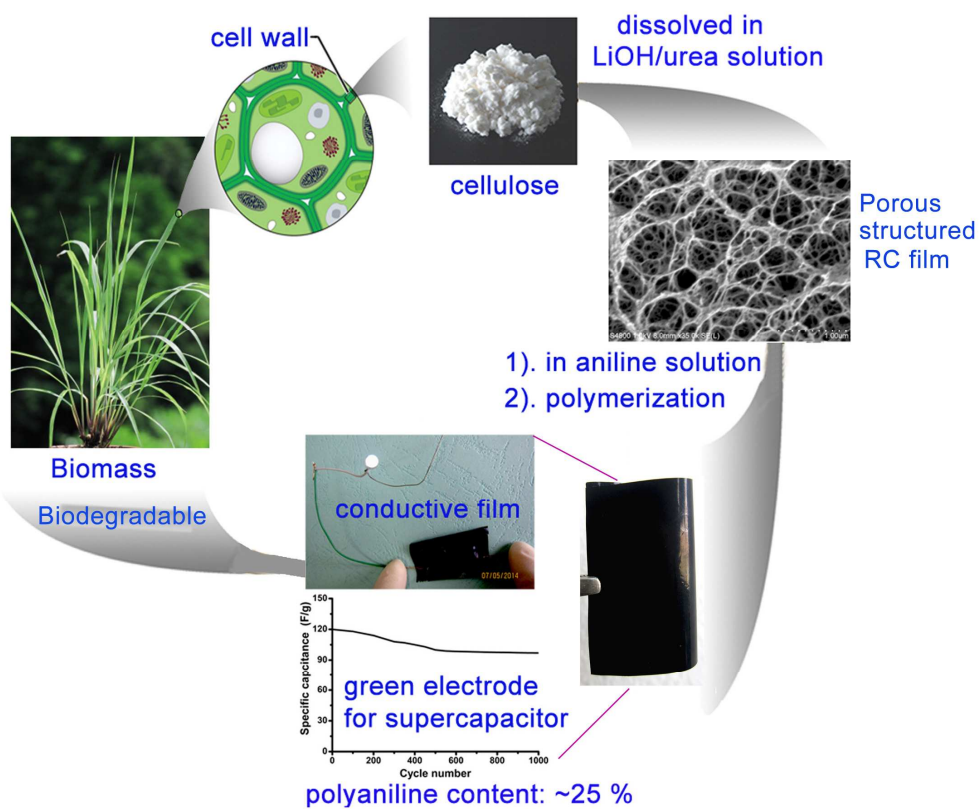
Fig. 10 Galvanostatic charge–discharge tests (a) and cyclic performance (b) of the RC/PA011 electrode in 6.0 mol•L^{-1} potassium hydroxide solution within the potential window of -0.2-0.8 V at a current density of 0.5 A• g^{-1}.

For table of content use only

The integration of cellulose with electronic elements could form green electronics with the merits of the biopolymer and conductive polymer.